Structures, magnetic and catalytic properties of three sandwich-type silicotungstates containing tetranuclear copper(II) clusters†

Fan Yu, Yu-Xiang Long, Yan-Ping Ren, Xiang-Jian Kong,* La-Sheng Long,* Rong-Bin Huang and Lan-Sun Zheng

Received 17th April 2010, Accepted 28th May 2010
First published as an Advance Article on the web 13th July 2010
DOI: 10.1039/c0dt00322k

Three sandwich-type silicotungstates, formulated as $[Cu_4(H_2O)_2(SiW_9O_{34})_2]\cdot 12NH_4\cdot 22H_2O$ (**1**), $[Cu_4(H_2O)_2(SiW_9O_{34})_2]\cdot 12NH_4\cdot 11H_2O$ (**2**) and $\{[Cu(NH_3)_4]_2[Cu(H_2O)_4][Cu_4(H_2O)_2(SiW_9O_{34})_2]\}$ $2[Cu(NH_3)_4(H_2O)]\cdot 2NH_4\cdot 6H_2O$ (**3**), were synthesized by microwave irradiation and hydrothermal reaction. Crystal structural analysis reveals that **1–3** possess the same dimeric polyoxoanions $[Cu_2SiW_9O_{34}(H_2O)]_2^{12-}$ featuring tetranuclear copper(II) clusters. Magnetic studies indicate that the Cu_4 clusters exhibit ferromagnetic coupling interactions. Investigation on their catalytic activity for the oxidation of ethylbenzene suggests that catalytic activity of **1–3** is closely related to the acidity of complexes and the existence of unsaturated coordination sites in the complex.

Introduction

Polyoxometalates (POMs), possessing tunable acidic and redox properties, are regarded as green catalysts and have been applied to several large-scale commercial processes.[1] Compared with the well-defined POMs, transition-metal-substituted polyoxometalates (TMSP) exhibit more promising catalytic properties due to the incorporation between transition metals and POMs, that is not available for POMs themselves, and their unique catalytic properties have been demonstrated in homogeneous catalytic reactions.[2]

As one of most notable subfamily in TMSP chemistry, the sandwich-type POMs have been attracting extensive interest in solid-state materials chemistry in the past several decades.[3–12] Since the first sandwich-type $[Co_4(H_2O)_2(\alpha\text{-B-}PW_9O_{34})_2]^{10-}$ POM was reported by Weakley *et al.* in 1973,[13] a number of sandwich-type POMs have been reported in the literature.[3–12] However, the investigation on the catalytic property of the sandwich-type TMSP remains scarce and few are focused on the mechanisms of heterogeneous catalysis.[14,15] Herein we report syntheses, structures, magnetic and catalytic properties of three Cu(II)-substituted polyoxometalates, namely, $[Cu_4(H_2O)_2(SiW_9O_{34})_2]\cdot 12NH_4\cdot 22H_2O$ (**1**), $[Cu_4(H_2O)_2(SiW_9O_{34})_2]\cdot 12NH_4\cdot 11H_2O$ (**2**) and $\{[Cu(NH_3)_4]_2$-$[Cu(H_2O)_4][Cu_4(H_2O)_2(SiW_9O_{34})_2]\}\cdot 2[Cu(NH_3)_4(H_2O)]\cdot 2NH_4\cdot$ $6H_2O$ (**3**). Complexes **1–3** possess the same dimeric polyoxoanions $[Cu_2SiW_9O_{34}(H_2O)]_2^{12-}$, which had been previously synthesized by Kortz *et al.*[16b]

State Key Laboratory of Physical Chemistry of Solid Surface and Department of Chemistry, College of Chemistry and Chemical Engineering, Xiamen University, Xiamen, 361005, China. E-mail: xjkong@xmu.edu.cn, lslong@xmu.edu.cn; Fax: +86 592 218 3047

† Electronic supplementary information (ESI) available: Fig. S1–S5. CCDC reference numbers 777446–777448. For ESI and crystallographic data in CIF or other electronic format see DOI: 10.1039/c0dt00322k

Experimental

Materials

Ethylbenzene was repurified before use. *tert*-Butyl hydroperoxide (TBHP) were purchased commercially. Other reagents used in the work were all AR grade.

Instrumentation

Atomic absorption results were obtained on Thermo Electron IRIS Intrepid II XSP. X-ray powder diffractometry (XRPD) was performed on Panalytical X-Pert pro diffractometer with Cu-Kα radiation (λ = 0.15418 nm, 40.0 kV, 30.0 mA). The reaction products of oxidation were determined and analyzed by a GC-920 instrument with a capillary column (30 m × 0.25 mm). The C, H and N microanalyses were carried out with a CE instrument EA 1110 elemental analyzer. TGA curves were measured on a SDT Q600 Thermal Analyzer. The microwave reactions were carried out using a CEM Discover. The magnetic measurements were carried out on crystalline powder samples with a Quantum Design MPMS XL-7 magnetometer working in dc mode. The experimental susceptibility data were corrected in order to obtain an approximately constant value of the $\chi_M T$ product at high temperatures (above 200 K). These corrections account for diamagnetism of the samples and temperature-independent paramagnetism (TIP) contributions.

Synthesis

$[Cu_4(H_2O)_2(SiW_9O_{34})_2]\cdot 12NH_4\cdot 22H_2O$ (1) and $\{[Cu(NH_3)_4]_2$-$[Cu(H_2O)_4][Cu_4(H_2O)_2(SiW_9O_{34})_2]\}\cdot 2[Cu(NH_3)_4(H_2O)]\cdot 2NH_4\cdot$ $6H_2O$ (3). 1.15 g Silicotungstic acid ($H_4SiW_{12}O_{40}$, 0.4 mmol), 0.05 g β-alanine (NH_2CH_2COOH, 0.5 mmol) and 0.148 g copper(II) nitrate ($Cu(NO_3)_2\cdot 6H_2O$, 0.5 mmol) were dissolved in 15 mL distilled water with stirring at room temperature. The pH value of the mixture was then adjusted to about 8 with 10% ammonia, the solution put into a 25 mL Teflon-lined Parr and heated to

160 °C for 24 h, and then cooled to 100 °C at a rate of 10 °C h^{-1}. After it was kept at 100 °C for 16 h, the mixture was cooled to room temperature at a rate of 3 °C h^{-1}. Purple crystals of **3** were obtained by filtration in 40% yield (based on Cu). Cyan crystals of **1** were obtained by slow evaporation of the filtrate solution for about one week in 30% yield (based on Cu). Calc. (found) for $Cu_4H_{96}N_{12}O_{92}Si_2W_{18}$ (**1**): H, 1.81 (1.58); N, 3.14 (3.12%). IR for **1** (KBr, cm^{-1}): 3441s, 3139s, 1628s, 1400vs, 1067w, 984w, 941m, 761s, 510m. Calc. (found) for $Cu_9H_{84}N_{18}O_{82}Si_2W_{18}$ (**3**): H, 1.50 (1.48); N, 4.51 (4.51%). IR (KBr, cm^{-1}) for **3**: 3432s, 3151s, 1618s, 1400s, 1264m, 983w, 942s, 879s, 758s, 509m.

$[Cu_4(H_2O)_2(SiW_9O_{34})_2]\cdot 12NH_4\cdot 11H_2O$ (2). 1.15 g Silicotungstic acid ($H_4SiW_{12}O_{40}$, 0.4 mmol), 0.05 g β-alanine (NH_2CH_2COOH, 0.5 mmol) and 0.148 g copper(II) nitrate ($Cu(NO_3)_2\cdot 6H_2O$, 0.5 mmol) were dissolved in 15 mL distilled water with stirring at room temperature. The pH value of the mixture was then adjusted to about 8 with 10% ammonia, then it was sealed in a microwave-specified 35 mL glass reactor and heated to 170 °C for 20 min at a microwave power of 80 W. Blue crystals of **2** were obtained by slow evaporation of the filtrate solution after about two weeks in 40% yield (based on $H_4SiW_{12}O_{40}$). Calc. (found) for $Cu_4H_{74}N_{12}O_{81}Si_2W_{18}$ (**2**): H, 1.45 (1.80); N, 3.26 (3.28%). IR (KBr, cm^{-1}): 3380s, 3151s, 1629s, 1400vs, 1237m, 933s, 874m, 815w, 790w, 705m, 533w, 495m.

X-Ray crystallography

Data collection was performed on a Bruker SMART Apex CCD diffractometer at 123 K for **1** and 273 K for **2**. Data for **3** were collected on an Oxford Gemini S Ultra using Mo-Kα radiation and equipped with an Oxford Instruments cryostat at 173 K. Absorption corrections were applied by using the multiscan program SADABS for **1** and **2**. The structures were solved by direct methods, and non-hydrogen atoms were refined anisotropically by least squares on F^2 using the SHELXTL program. Crystal data as well as details of data collection and refinement for **1–3** are summarized in Table 1.

Catalytic reaction

Oxidation reactions of ethylbenzene was carried out in a RB flask fitted with a water-cooled condenser by using 70 wt% aqueous *tert*-butyl hydroperoxide (TBHP) as an oxidant in acetonitrile. The reaction mixture was centrifuged to remove the catalyst and analyzed by gas chromatography using a flame-ionization detector (FID). Assignments were made by comparison with authentic samples analyzed under the same conditions.

Results and discussion

Description of crystal structures

Crystal structural analysis reveals that **1** consists of one sandwich Cu_4-substituted polyoxoanion $[Cu_4(H_2O)_2(SiW_9O_{34})_2]^{12-}$, 12 dissociative NH_4^+ cations and 22 crystallization water molecules. The polyoxoanion $[Cu_4(H_2O)_2(SiW_9O_{34})_2]^{12-}$ anion has the general sandwich structure of the series $[M_4(H_2O)_2(SiW_9O_{34})_2]^{12-}$ (M = Co^{2+}, Cu^{2+}, Zn^{2+}, Mn^{2+}, Ni^{2+}).[16] As shown in Fig. 1a, two trilacunary α-B-$[SiW_9O_{34}]^{10-}$ Keggin moieties were linked through a tetrametallic unit Cu_4O_{16}, leading to the sandwich-type $[Cu_4(H_2O)_2(SiW_9O_{34})_2]^{12-}$ anion. The Cu–O bond lengths are in the range of 1.935(11)–2.516(15) Å for Cu1 and 1.934(11)–2.418(11) Å for Cu2 (Table 2). The range of O–Cu–O angles are 88.0(5)–94.3(5)° for Cu1 and 83.3(5)–94.5 (5)° for Cu2, respectively, comparable to these of 1.960(10)–2.416(10) Å and 91.2(4)–96.2(5)° in $K_3Na_5[Cu_4(H_2O)_2(SiW_9O_{34})_2]\cdot 26H_2O$.[16b]

Complex **2** is almost isostructural to complex **1**, except for the number of guest water molecules (Fig. 1b). The Cu–O bond lengths are 1.965(10)–2.451(14) Å for Cu1 and 1.948(10)–2.468(19) Å for Cu2.

Table 1 Crystal data as well as details of data collection and refinement for **1**, **2** and **3**

	1	2	3
Formula	$Cu_4H_{96}N_{12}O_{92}Si_2W_{18}$	$Cu_4H_{74}N_{12}O_{81}Si_2W_{18}$	$Cu_9H_{84}N_{18}O_{82}Si_2W_{18}$
M_r	5356.53	5158.35	5586.19
Crystal system	Monoclinic	Monoclinic	Triclinic
Space group	$P2_1/n$	$P2_1/n$	$P\bar{1}$
a/Å	16.396(2)	12.792(3)	12.4289(5)
b/Å	13.812(2)	20.277(4)	12.8045(4)
c/Å	19.875(3)	16.384(3)	16.2673(5)
α/°	90	90	83.324(3)
β/°	112.518(2)	105.476(4)	73.451(3)
γ/°	90	90	61.870(4)
V/Å^3	4157.7(10)	4095.7(14)	2188.01(13)
Z	2	2	1
D_c/g cm^{-3}	4.279	4.183	4.240
μ/mm^{-1}	25.948	26.323	25.828
R_{int}	0.0744	0.0991	0.0429
Data/params	7208/577	7114/541	7506/583
θ/°	1.85–25.00	1.63–25.00	2.20–25.00
Obsd reflns	6270	4996	6531
R_1 $[I > 2\sigma(I)]^a$	0.0586	0.0670	0.0619
wR_2 (all data)^b	0.1502	0.1710	0.1665

^{a} $R_1 = \sum||F_o| - |F_c||/\sum|F_o|$. ^{b} $wR_2 = \{\sum[w(F_o^2 - F_c^2)^2]/\sum[w(F_o^2)^2]\}^{1/2}$.

Table 2 Selected bond lengths (Å) and angles (°) within the Cu_4O_{16} units of **1–3**[a], $K_3Na_5[Cu_4(H_2O)_2(SiW_9O_{34})_2]\cdot 26H_2O$ (**4**)[b] and $K_8Na_2[Cu_4(H_2O)_2(PW_9O_{34})_2]\cdot 16H_2O$ (**5**);[c] X = Si (**1–4**) or P (**5**); Cu···Cu interactions (Å) and magnetic exchange interactions J (cm^{-1})

	1	2	3	4	5
Cu1–O(W1)	1.949(12)	2.015(10)	1.949(7)	1.984(12)	1.94(1)
Cu2–O(W1)	2.420(11)	1.987(11)	2.449(9)	2.416(10)	2.36(1)
Cu1–O(X)	2.416(10)	1.999(10)	2.396(6)	2.414(11)	2.55(1)
Cu1–O(W2)	1.931(11)	2.452(11)	1.957(5)	1.960(10)	1.96(1)
Cu2–O(X)	2.006(11)	1.998(9)	1.981(7)	1.991(10)	2.05(1)
Cu1–O(W1)–Cu2	91.6(4)	96.7(4)	89.0(8)	91.4(4)	97.6
Cu1–O(X)–Cu2	90.3(4)	96.9(6)	89.8(2)	91.2(4)	89.2
Cu1–O(W2)–Cu2A	93.0(4)	93.7(6)	90.2(2)	92.5(4)	98.2
Cu1–O(X)–Cu2A	91.3(4)	92.4(8)	89.7(2)	91.2(4)	89.6
Cu2–O(X)–Cu2A	96.7(5)	90.7(7)	96.7(2)	96.2(5)	97.6
Cu1···Cu2	3.149(3)	2.990(3)	3.105(2)	3.162(3)	3.246(4)
Cu1···Cu2A	3.162(3)	3.242(3)	3.113(2)	3.163(3)	3.263(4)
Cu2···Cu2A	2.982(4)	3.196(3)	2.975(2)	2.965(4)	3.087(4)
Cu1···Cu1A	5.562(8)	5.356(3)	5.460(7)	5.588(5)	5.724
J_1	0.22	0.34	0.03	–0.10(2)	–3.5
J_2	9.13	9.31	9.76	–0.29(2)	–12.5

[a] This work. [b] Ref. 16*b*. [c] Ref. 15*b* and 16*c*.

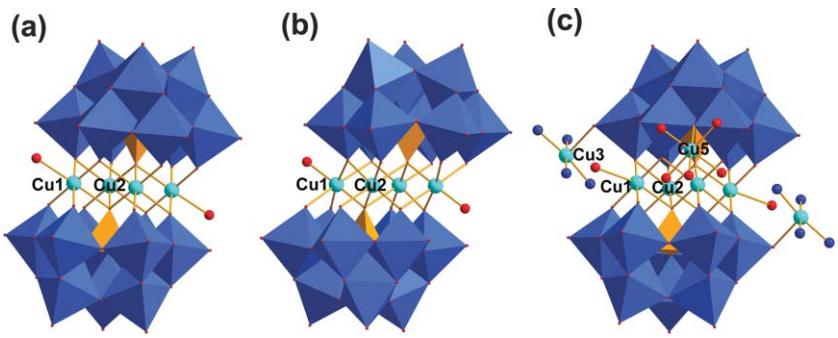

Fig. 1 Plots of (a) $\{Cu_4(H_2O)_2(SiW_9O_{34})_2\}^{12-}$ for **1**; (b) $\{Cu_4(H_2O)_2(SiW_9O_{34})_2\}^{12-}$ for **2** and (c) $\{[Cu(NH_3)_4]_2[Cu(H_2O)_4][Cu_4(H_2O)_2(SiW_9O_{34})_2]\}^{6-}$ for **3**.

Complex **3** contains one sandwich-type $[Cu_4(H_2O)_2(SiW_9O_{34})_2]^{12-}$ anion, two $[Cu(NH_3)_4]^{2+}$ cations, one $[Cu(H_2O)_4]^{2+}$ cation, two dissociative $[Cu(NH_3)_4(H_2O)]^{2+}$ cations, two NH_4^+ cations and eight guest water molecules. As shown in Fig. 1c, the $[Cu_4(H_2O)_2(SiW_9O_{34})_2]^{12-}$ anion has a similar structure to the sandwich-type polyoxoanion in **1**. Each of the $[Cu_4(H_2O)_2(SiW_9O_{34})_2]^{12-}$ anions in **3** also connects two $[Cu(NH_3)_4]^{2+}$ cations and one $[Cu(H_2O)_4]^{2+}$ cation, forming a $\{[Cu(NH_3)_4]_2[Cu_4(H_2O)_2(SiW_9O_{34})_2]\}^{8-}$ unit. The "Z"-shaped 1D chain structure of **3** can be viewed in terms of adjacent $\{[Cu(NH_3)_4]_2[Cu_4(H_2O)_2(SiW_9O_{34})_2]\}^{8-}$ units linked by sharing the $[Cu(H_2O)_4]^{2+}$ cation with a Cu–O distance of 2.776(9) Å, as shown in Fig. 2. Two isolated $[Cu(NH_3)_4(H_2O)]^{2+}$ and two NH_4^+ cations acting as counter-cations are hydrogen-bonded to the $\{[Cu(NH_3)_4]_2[Cu(H_2O)_4][Cu_4(H_2O)_2(SiW_9O_{34})_2]\}^{6-}$ anion. Overall, there are four five-coordinated Cu^{2+} ions in **3**. The Cu–O and Cu–N distances in **3** are in range 1.902(7)–2.776(9) and 1.930(14)–2.049(8) Å, respectively.

Magnetic properties of 1, 2 and 3

The magnetic properties of **1**, **2** and **3** are investigated through magnetization measurements at 2 K and variable-temperature susceptibility measurements over the temperature range of 2–300 K with an applied magnetic field of 5000 Oe. Owing to the spin quantum number of W(VI) ion being zero, the magnetic properties of **1–3** are ascribed to the contribution of Cu(II) ions. The field dependence of magnetizations and $\chi_M T$ *vs.* T plots for **1–3** are shown in Fig. 3.

For **1** and **2**, the observed magnetization increases steeply and reach saturated values of about 3.84 and 3.68 $N\beta$ at 3 T, respectively, which are in accordance with the values predicted from the Brillouin function for four Cu(II) ions with $g = 2.0$ ($M = 4 \times (2 \times 1/2) = 4$), and indicate the possibility of the existence of ferromagnetic interactions within the Cu_4 units; however, for **3**, the magnetization shows a slow increase and reaches a quasi-saturated value of 8.62 $N\beta$ at 7 T, in line with the expected value for a Cu_4 unit and five isolated Cu(II).

The $\chi_M T$ values of **1** and **2** at room temperature are 1.53 and 1.51 $cm^3\ mol^{-1}\ K$, which are consistent with the value 1.500 $cm^3\ mol^{-1}\ K$ expected for four independent Cu(II) ions in the molecule. The values of $\chi_M T$ increase gradually as the temperature is lowered and reach a maximum values of 2.00 and 2.1 $cm^3\ mol^{-1}\ K$ at 2 K, indicating weak ferromagnetic interactions between the Cu(II) ions. For **3**, due to the existence of isolated Cu(II), the temperature dependence of the magnetic susceptibility of **3** shows

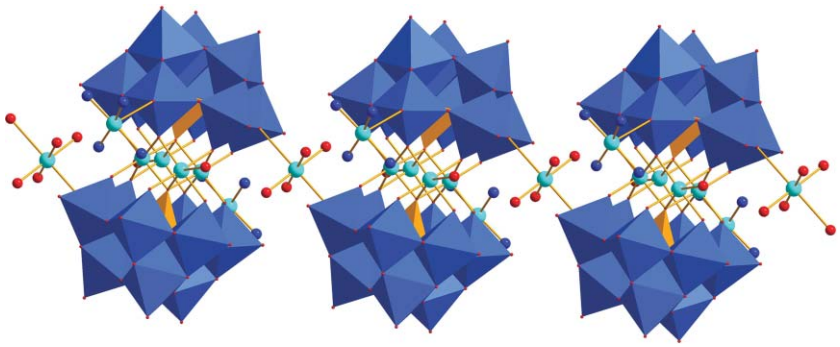

Fig. 2 Plot of the "Z"-shaped 1D chain structure in **3**.

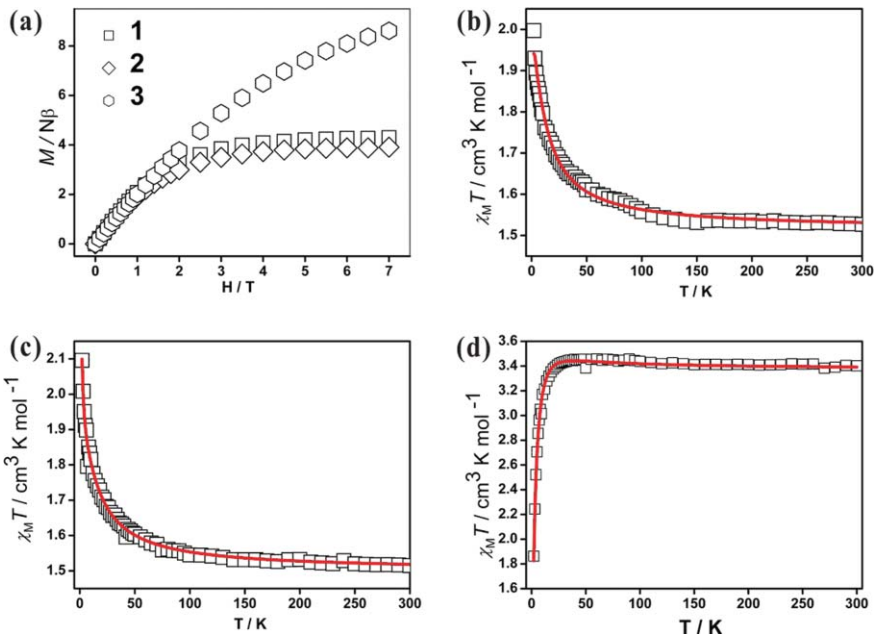

Fig. 3 (a) The field dependence of the magnetization for **1**, **2** and **3** and plots of $\chi_M T$ *vs.* T for **1** (b), **2** (c) and **3** (d) (the solid lines are the best fit to the experimental data).

an almost constant value around 3.43 $cm^3\ mol^{-1}\ K$ from 300 to 20 K, which is in line with the value for nine independent Cu(II) ions. Below 20 K, the $\chi_M T$ values decrease abruptly and reach 1.88 $cm^3\ mol^{-1}\ K$ at 2 K, which is indicative of either intra- and/or intermolecular antiferromagnetic interactions between the spin carriers of isolated Cu(II).[17]

In the Cu_4 unit, the magnetism could be determined by the existence of different Cu–O bond distances, Cu–O–Cu angles and Cu–Cu distances. In order to analyze the magnetism, the exchange model (shown as Scheme 1) is established in which the transition metal ions, Cu1, Cu2, Cu1A and Cu2A, are represented as 1, 2, 3 and 4 respectively. The spin Hamiltonian (1) for the tetrameric cluster which includes the effect of metal ions 1–4 is used to fit the magnetism of these compounds:

$$\hat{H} = g\mu_B(m + m')H - 2J_2S_2S_4 - 2J_1(S_1S_2 + S_1S_4 + S_2S_3 + S_3S_4) \quad (1)$$

where, $g = 2.00$,[18] μ_B is the Bohr magneton, H is the external magnetic field, and J_1 and J_2 refer to the magnetic exchange

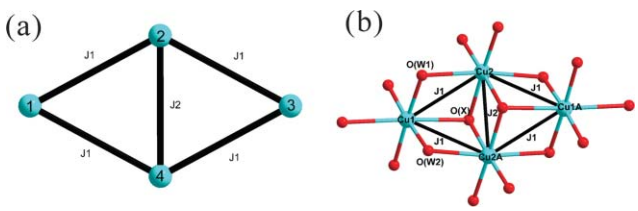

Scheme 1 (a) The exchange model used to analyze the magnetism; (b) ball-and-stick representation of the Cu_4O_{16} fragment of **1–3**.

interactions of the four sides and shortest diagonal of the rhombus according to the numbering scheme.

The eigenvalues for the above Hamiltonian can be derived from the vector coupling method of Kambé:[16b,19]

$$\hat{H} = -J_2[S_{24}(S_{24} + 1) - S_2(S_2 + 1) - S_4(S_4 + 1)] - J_1[S_T(S_T + 1) - S_{13}(S_{13} + 1) - S_{24}(S_{24} + 1)] \quad (2)$$

where $S_T = S_{13} + S_{24}$, with $S_{13} = S_1 + S_3$ and $S_{24} = S_2 + S_4$, and $S_1 = S_2 = S_3 = S_4 = 1/2$ for Cu(II). However, for **3**, the contribution of isolated Cu(II) ions must be considered as reported.[19] All of the fitting processes were performed using the MAGPACK package.[20]

The magnetic susceptibility data for **1**, **2** and **3** were least-squares fit to this model (Fig. 3) without the consideration of interaction between adjacent Cu_4 units ($zJ = 0$). Fitting of the magnetic susceptibility data in the temperature range of 2–300 K give $g = 2.01$, $J_1 = 0.22$ cm^{-1} and $J_2 = 9.13$ cm^{-1} for **1**; $g = 1.95$, $J_1 = 0.34$ cm^{-1} and $J_2 = 9.31$ cm^{-1} for **2**; $g = 2.05$, $J_1 = 0.03$ cm^{-1}, and $J_2 = 9.76$ cm^{-1} for **3**. These fitted values are much lower than the values obtained from the ferromagnetic coupling Cu_6 cores reported previously.[21] However, it is clear that weak ferromagnetic coupling occurs between Cu1–Cu2 and Cu2–Cu2A, especially efficient coupling along the short diagonal which might be a result of the Jahn–Teller distorted Cu(II) ions.[15] The unusual presence of ferromagnetic coupling in **1–3** is ascribed to the narrow Cu–O–Cu angles in the Cu_4O_{16} units in the range of 90–97° (Table 2), which suggests the possibility of an explanation based on orthogonality of the magnetic orbitals through the bridging oxygen atoms.[22]

It is interesting that the Cu_4O_{16} clusters in **1–3** exhibit ferromagnetic exchange coupling, which is different from the antiferromagnetic exchange interactions in $K_3Na_5[Cu_4(H_2O)_2(SiW_9O_{34})_2]\cdot 26H_2O$ (**4**) and $K_8Na_2[Cu_4(H_2O)_2(PW_9O_{34})_2]\cdot 16H_2O$ (**5**), reported by Kortz *et al.*[16b] and Coronado *et al.*,[15b,16c] respectively. The observed differences in the magnetic properties of **1–3** compared with **4** and **5** should be predominantly due to differences in the geometry of the cental Cu_4O_{16} units. As shown in Table 2, for **1**, the Cu1–O(W1) and Cu1–O(W2) bond lengths are slightly shorter than those of **4** and **5**; for **2**, the Cu2–O(W1) and Cu1–O(X) bond lengths are significantly shorter, and the Cu2–O(X)–Cu2A angles are significantly smaller than that of **4** and **5**; For **3**, the Cu–O–Cu bond angles are obviously smaller than those of **4** and **5**. As a result, the Cu···Cu distances in **1–3** are slightly shorter than those of **4** and **5**, and it could be expected that **1–3** exhibit the ferromagnetic exchange coupling.

From the magnetic point of view, these unusual ferromagnetic results give essential information about magnetic coupling in polyoxometalate chemistry. Further experimental work is required to establish the ideal model for the study of the exchange interactions in highly symmetrical clusters of increasing nuclearities and controlled magnetic couplings.[23]

Catalytic properties

Selective oxidation of ethylbenzene (Scheme 2) catalyzed by **1–3** was carried out under the same reaction conditions as previously reported,[24a] so as to reveal the relationship between structure and catalytic properties. A comparative experiment without catalyst performed under otherwise identical conditions gave negligible conversion.

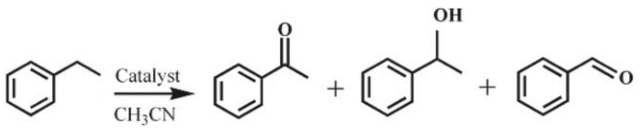

Scheme 2 Oxidation of ethylbenzene to acetophenone.

As shown in Fig. 4, the major product of oxidation of ethylbenzene (EB) was acetophenone (AP) with a small amount of 1-phenylethanol (PE) and benzaldehyde (BA). The conversion for the oxidation of ethylbenzene for **1** and **2** increased slowly during the whole reaction process and reached 26.1 and 15.3% (Fig. 4a and 4b), respectively, when extending the reaction time to 10 h. Different from that of **1** and **2**, the conversion for the oxidation of ethylbenzene for **3** increased substantially and reached 49.4%, and the selectivity for acetophenone was 81.9% (Fig. 4c), when the reaction was performed for 3 h. On prolonging the reaction time to 10 h, the conversion only increased slowly (55.5%, Fig. 4c), but the selectivity for acetophenone significantly increased and reached 88.9% (Table 3). These results indicate that the catalytic activity of **3** for the oxidation of ethylbenzene is significantly higher than that of **1** and **2**.

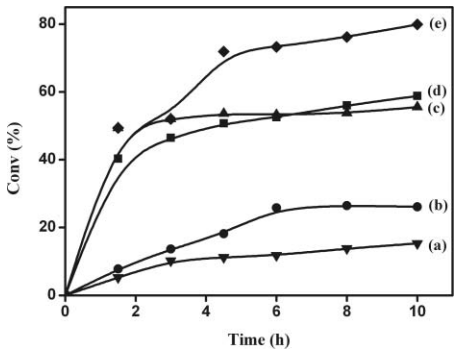

Fig. 4 Effect of the reaction time on the behaviour of ethylbenzene oxidation at 343 K with catalysts **1** (a), **2** (b), **3** (c, e) and **4** (d). *Reaction conditions* for (a)–(d): ethylbenzene (0.3 mL, 2.44 mmol), catalyst (0.005 mmol), 70% TBHP (0.75 mL, 4.88 mmol), acetonitrile (8 mL); *Reaction conditions* for (e): ethylbenzene (0.3 mL, 2.44 mmol), catalyst (0.005 mmol), 70% TBHP (1.50 mL, 9.76 mmol), acetonitrile (8 mL).

Clearly, the difference in catalytic property between **1** (or **2**) and **3** is related to that of their structures. Based on their crystal structural analysis, the main differences between **1** (or **2**) and **3** are that of: (1) the acidity (**1** and **2** contain twelve NH_4^+ cations, while **3** only contains two NH_4^+ cations); (2) the amount of copper(II) ions (**1** and **2** contain four copper(II) ions, while **3** contains nine copper(II) ions); (3) the coordination number of copper(II) ions (**1** and **2** contain four six-coordinated copper

Table 3 Effect of different catalysts on the oxidation of ethylbenzene and product selectivity upon reaction for 10 h

			Selectivity[d] (%)			
Catalyst	T/K	Conv.[c] (%)	AP	BA	PE	other
1[a]	343	26.1	72.3	4.4	18.7	4.5
2[a]	343	15.3	71.7	4.3	20.7	4.3
3[a]	343	55.5	88.9	5.2	3.9	2.0
3[b]	343	79.9	93.6	3.9	1.2	1.3
4[a]	343	58.8	88.0	3.3	7.0	1.7
Blank	343	6.6	—	—	—	—

[a] *Reaction conditions*: ethylbenzene (0.3 mL, 2.44 mmol), catalyst (0.005 mmol), 70% TBHP (0.75 mL, 4.88 mmol), acetonitrile (8 mL), time: 10 h; [b] *Reaction conditions*: ethylbenzene (0.3 mL, 2.44 mmol), catalyst (0.005 mmol), 70% TBHP (1.50 mL, 9.76 mmol), acetonitrile (8 mL), reaction time: 10 h, [c] Average conversion of two runs based on GC results. The reaction mixture was analyzed twice, before and after treatment with PPh_3, and no differences were observed. The carbon balance was also evaluated and found to be generally better than 93%. [d] Ethylbenzene (EB) conversion (%) defined as: $100(n_{AP} + n_{BA} + n_{PE} + n_{other})/n_{EB0}$; acetophenone (AP) selectivity (%) defined as $100n_{AP}/(n_{AP} + n_{BA} + n_{PE} + n_{other})$ (n_{EB0}: initial mol of ethylbenzene); other products (mainly benzoic acid) have negligible yield in the reaction.

ions, while **3** contains four five-coordinated copper ions and five six-coordinated copper ions). As a previous study for such a heterogeneous oxidation reaction demonstrated that the difference in the amount of copper(II) is not the key factor influencing the catalytic properties,[24] we investigated the effect of the acidity on their catalytic property by selecting a known complex, $K_3Na_5[\{SiCu_2W_9O_{34}(H_2O)\}_2]\cdot 26H_2O$ (**4**),[16b] not containing NH_4^+ and testing it under identical conditions as for **1–3**. As shown in Fig. 4d, the conversion for the oxidation of ethylbenzene for **4** increased during the whole process and reached about 60%, significantly higher than that of **1** and **2**, and slightly higher than that of **3**, at the reaction time of 10 h. This result indicates that acidity of the catalyst is an important factor influencing the oxidation of the ethylbenzene, which is consistent with previous results.[24a] It was noted that, although the conversion for the oxidation of ethylbenzene for **4** is slightly higher than that for **3** at the reaction time of 10 h, it is invariably lower than that for **3** when the reaction time is less than 6 h. This fact implies that there must exist another factor influencing the catalytic property of the complex, besides its acidity. Probably, the unsaturated coordination sites (five-coordinated copper(II) ions) in **3** lead to the difference in the catalytic property. Consistently, GC analysis showed that the TBHP was consumed for **3** when the reaction time was 3 h, while it was not used up for **1**, **2** and **4** for reaction time up to 10 h. Thus, the catalytic property of **3** for the oxidation reaction was also performed at the condition of ratio of TBHP to substrate = 4 : 1. Under otherwise identical conditions, ethylbenzene conversion was obviously enhanced and reached 71.9% at 4.5 h (Fig. 4e). Increasing the reaction time to 10 h leads to the conversion up to 80% (Table 3) and the selectivity of acetophenone rose to 93.6%. The significant increase of the ethylbenzene conversion for **3** indicates that the unsaturated coordination sites favor enhancement of catalytic activity, consistent with previous results.[25] This is understandable, since *tert*-butyl hydroperoxide is activated by coordinating with metal oxide and metal centres.[26,27] When the catalyst has a vacant site, the *t*-BuOO$^{\bullet}$ radical can coordinate its O donor to the vacant site to form the intermediate {*t*-BuO–O–Cu} during the reaction,[26,27] which favors complete oxidation of ethylbenzene to produce the desired product.

The filtrate was catalytically inactive for the oxidation reaction after **3** was removed from the reaction solution, suggesting that the catalytic process is truly heterogeneous. The amount of metal ions in the reaction filtrate was tested by atomic absorption spectra and no copper species (<0.1 ppm) was detected in the product solution, indicating that the oxidation process is catalyzed by the solid-state complex. The XPRD of the fresh catalyst and that after the second cycle were measured and both showed almost identical diffraction patterns (Fig. S2–S4, ESI†), indicating that the structural integrity of **1–3** was maintained during the reaction.[27] We also evaluated the reusability of catalyst **3**, which was recycled once in the oxidation of ethylbenzene, with no significant loss of catalytic activity observed (Fig. S5, ESI†). Therefore, **3** was stable in acetonitrile and could be reused with retention of its high catalytic activity and selectivity.

Conclusions

In summary, we have prepared three sandwich-type silicotungstates containing tetranuclear copper(II) clusters. Magnetic study shows that the three complexes exhibit weak ferromagnetic coupling interactions. Investigation on their catalytic activity for the oxidation of ethylbenzene demonstrates that the acidity of the complexes significantly influences their catalytic activity, and the existence of the unsaturated coordination sites in the complex would enhance its catalytic activity for the oxidation reaction.

Acknowledgements

We thank the NNSFC (Grant Nos. 20825103, 20721001 and 90922031), the 973 Project from MSTC (Grant 2007CB815304) and the Natural Science Foundation of Fujian Province of China (Grant No. 2008J0010).

Notes and references

1 V. W. Day and W. G. Klemperer, *Science*, 1985, **228**, 533; Q. Chen and J Zubieta, *Coord. Chem. Rev.*, 1992, **114**, 107; S. K. Saha, M. Ali and P. Banerjee, *Coord. Chem. Rev.*, 1993, **122**, 41; N. Mizuno and M. Misono, *J. Mol. Catal.*, 1994, **86**, 319; C. L. Hill and C. M. Prosser-McCartha, *Coord. Chem. Rev.*, 1995, **143**, 407.

2 R. Neumann and C. Abu-Gnim, *J. Chem. Soc., Chem. Commun.*, 1989, 1324; R. Neumann and C. Abu-Gnim, *J. Am. Chem. Soc.*, 1990, **112**, 6025; N. Mizuno, M. Tateishi, T. Hirose and M. Iwamoto, *Chem. Lett.*, 1993, 1985; N. Mizuno, T. Hirose, M. Tateishi and M. Iwamoto, *Chem. Lett.*, 1993, 1839; R. Neumann and M. Dahan, *J. Chem. Soc., Chem. Commun.*, 1995, 171; O. A. Kholdeeva, V. A. Grigoriev, G. M. Maksimov, M. A. Fedotov, A. V. Golovin and K. I. Zamareav, *J. Mol. Catal. A: Chem.*, 1996, **114**, 123; V. Indira, P. A. Joy, S. Gopinathan and C. Gopinathan, *Indian J. Chem., Sect. A*, 1998, **37**, 473; D. Kumar, E. Derat, A. M. Khenkin, R. Neumann and S. Shaik, *J. Am. Chem. Soc.*, 2005, **127**, 17712; A. R. Howells, A. Sankarraj and C. Shannon, *J. Am. Chem. Soc.*, 2004, **126**, 12258.

3 M. T. Pope, *Heteropoly and Isopoly Oxometalates*, Springer-Verlag, Berlin, 1983.

4 C. L. Hill, (editor), *Chem. Rev.*, 1998, **98**(1): special issue on POMs; E. Coronado, C. Giménez-Saiz and C. J. Gómez-García, *Coord. Chem. Rev.*, 2005, **249**, 1776; D. L. Long, E. Burkholder and L. Cronin, *Chem. Soc. Rev.*, 2007, **36**, 105; T. Akutagawa, D. Endo, S. I. Noro, L. Cronin and T. Nakamura, *Coord. Chem. Rev.*, 2007, **251**, 2547.

5 U. Kortz, N. K. Al-Kassem, M. G. Savelieff, N. A. Al Kadi and M. Sadakane, *Inorg. Chem.*, 2001, **40**, 4742; L. Ruhlmann, J. Canny, R. Contant and R. Thouvenot, *Inorg. Chem.*, 2002, **41**, 3811; B. S. Bassil, M. H. Dickman and U. Kortz, *Inorg. Chem.*, 2006, **45**, 2394; S. Nellutla, J. van Tol, N. S. Dalal, L. H. Bi, U. Kortz, B. Keita, L. Nadjo, G. A. Khitrov and A. G. Marshall, *Inorg. Chem.*, 2005, **44**, 9795; C. M. Tourné, G. F. Tourné and F. Zonnevijlle, *J. Chem. Soc., Dalton Trans.*, 1991, 143; Z. Zhang, Y. Li, E. Wang, X. Wang, C. Qin and H. An, *Inorg. Chem.*, 2006, **45**, 4313.

6 J. W. Zhao, H. P. Jia, J. Zhang, S. T. Zheng and G. Y. Yang, *Chem.–Eur. J.*, 2007, **13**, 10030; J. W. Zhao, B. Li, S. T. Zheng and G. Y. Yang, *Cryst. Growth Des.*, 2007, **7**, 2658; L. Fan, E. Wang, Y. Li, H. An, D. Xiao and X. Wang, *J. Mol. Struct.*, 2007, **841**, 28; J. W. Zhao, J. Zhang, S. T. Zheng and G. Y. Yang, *Chem. Commun.*, 2008, 570; J. W. Zhao, C. M. Wang, J. Zhang, S. T. Zheng and G. Y. Yang, *Chem.–Eur. J.*, 2008, **14**, 9223; J. W. Zhao, S. T. Zheng, Z. H. Li and G. Y. Yang, *Dalton Trans.*, 2009, 1300; J. P. Wang, X. D. Du and J. Y. Niu, *Chem. Lett.*, 2006, **35**, 1408; J. P. Wang, J. Du and J. Y. Niu, *CrystEngComm*, 2008, **10**, 972; S. Z. Li, J. W. Zhao, P. T. Ma, J. Du, J. Y. Niu and J. P. Wang, *Inorg. Chem.*, 2009, **48**, 9819; J. P Wang, P. T. Ma, Y. Shen and J. Y. Niu, *Cryst. Growth Des.*, 2008, **8**, 3130.

7 P. Mialane, A. Dolbecq, J. Marrot, E. Rivière and F. Sécheresse, *Angew. Chem., Int. Ed.*, 2003, **42**, 3523; M. Sadakane, M. H. Dickman and M. T. Pope, *Angew. Chem., Int. Ed.*, 2000, **39**, 2914; A. Dolbecq, J.-D. Compain, P. Mialane, J. Marrot, E. Rivière and F. Sécheresse, *Inorg. Chem.*, 2008, **47**, 3371.

8 P. Mialane, A. Dolbecq, J. Marrot, E. Rivière and F. Sécheresse, *Chem.–Eur. J.*, 2005, **11**, 1771; C. Pichon, A. Dolbecq, P. Mialane, J. Marrot,

E. Rivière, M. Zynek, T. McCormac, S. A. Borshch, E. Zueva and F. Sécheresse, *Chem.–Eur. J.*, 2008, **14**, 3189.
9 S. S. Mal and U. Kortz, *Angew. Chem., Int. Ed.*, 2005, **44**, 3777.
10 U. Kortz, F. Hussian and M. Reicke, *Angew. Chem., Int. Ed.*, 2005, **44**, 3773.
11 B. Z. Lin, L. W. He, B. H. Xu, X. L. Li, Z. Li and P. D. Liu, *Cryst. Growth Des.*, 2009, **9**, 273; H. Liu, C. Qin, Y. G. Wei, L. Xu, G. G. Gao, F. Y. Li and X. S. Qu, *Inorg. Chem.*, 2008, **47**, 4166.
12 Z. Luo, P. Kögerler, R. Cao and C. L. Hill, *Inorg. Chem.*, 2009, **48**, 7812; P. Mialane, C. Duboc, J. Marrot, E. Rivière, A. Dolbecq and F. Sécheresse, *Chem.–Eur. J.*, 2006, **12**, 1950; M. J. Manos, A. J. Tasiopoulos, E. J. Tolis, N. Lalioti, J. Derek Woollins, A. M. Z. Slawin, M. P. Sigalas and T. A. Kabanos, *Chem.–Eur. J.*, 2003, **9**, 695; H. Andres, J. M. Clemente-Juan, M. Aebersold, H. U. Güdel, E. Coronado, H. Büttner, G. Kearly, J. Melero and R. Burriel, *J. Am. Chem. Soc.*, 1999, **121**, 10028; J. M. Clemente-Juan, H. Andres, J. J. Borrás-Almenar, E. Coronado, H. U. Güdel, M. Aebersold, G. Kearly, H. Büttner and M. Zolliker, *J. Am. Chem. Soc.*, 1999, **121**, 10021; B. S. Bassil, U. Kortz, A. S. Tigan, J. M. Clemente-Juan, B. Keita, P. Oliveira and L. Nadjo, *Inorg. Chem.*, 2005, **44**, 9360.
13 T. J. R. Weakley, H. T. Evans Jun, J. S. Showell, G. F. Tourné and C. M. Tourné, *J. Chem. Soc., Chem. Commun.*, 1973, 139.
14 P. Liu, C. H. Wang and C. Li, *J. Catal.*, 2009, **262**, 159; P. Liu, H. Wang, Z. C. Feng, P. L. Ying and C. Li, *J. Catal.*, 2008, **256**, 345; J. T. Rhule, W. A. Neiwert, K. I. Hardcastle, B. T. Do and C. L. Hill, *J. Am. Chem. Soc.*, 2001, **123**, 12101.
15 (*a*) N. Casañ-Pastor, J. Bas-Serra, E. Coronado, G. Pourroy and L. C. W. Baker, *J. Am. Chem. Soc.*, 1992, **114**, 10380; (*b*) C. J. Gómez-García, E. Coronado and J. J. Borrás-Almenar, *Inorg. Chem.*, 1992, **31**, 1667.
16 (*a*) C. J. Gómez-García, J. J. Borrás-Almenar, E. Coronado and L. Ouahab, *Inorg. Chem.*, 1994, **33**, 4016; (*b*) U. Kortz, S. Isber, M. H. Dickman and D. Ravot, *Inorg. Chem.*, 2000, **39**, 2915; (*c*) J. M. Clemente-Juan and E. Coronado, *Coord. Chem. Rev.*, 1999, **193–195**, 361.
17 J. Long, L. M. Chamoreau, C. Mathonière and V. Marvaud, *Inorg. Chem.*, 2009, **48**, 22.
18 R. L. Carlin, *Magnetochemistry*, Springer-Verlag, New York, 1986, ch. 4 and 5.
19 W. L. Gladfelter, M. W. Lynch, W. P. Schaefer, D. N. Hendrickson and H. B. Gray, *Inorg. Chem.*, 1981, **20**, 2390.
20 (*a*) J. J. Borrás-Almenar, J. M. Clemente-Juan, E. Coronado and B. S. Tsukerblat, *J. Comput. Chem.*, 2001, **22**, 985; (*b*) G. L. Zhuang, X. J. Sun, L. S. Long, R. B. Huang and L. S. Zheng, *Dalton Trans.*, 2009, 4640.
21 S. T. Zheng, D. Q. Yuan, J. Zhang and G. Y. Yang, *Inorg. Chem.*, 2007, **46**, 4569.
22 R. D. Willett, D. Gatteschi, and O. Kahn, *Magnetostructural Correlations in Exchange Coupled Systems*, NATO, Advanced Studies Ser. C, Vol. 140, Reidel, Dordrecht, 1985.
23 J. M. Clemente-Juan, E. Coronado, J. R. Galán-Mascarós and C. J. Gómez-García, *Inorg. Chem.*, 1999, **38**, 55.
24 (*a*) F Yu, X. J. Kong, Y. Y. Zheng, Y. P. Ren, L. S. Long, R. B. Huang and L. S. Zheng, *Dalton Trans.*, 2009, 9503; (*b*) K. O. Xavier, J. Chacko and K. K. Mohammed Yusuff, *Appl. Catal., A*, 2004, **258**, 251–259; (*c*) T. H. Bennur, D. Srinivas and S. Sivasanker, *J. Mol. Catal. A: Chem.*, 2004, **207**, 163–171; (*d*) M. Salavati-Niasari, *J. Mol. Catal. A: Chem.*, 2008, **284**, 97–107.
25 A. M. Kirillov, M. N. Kopylovich, M. V. Kirillova, M. Haukka, M. F. C. Guedes da Silva and A. J. L. Pombeiro, *Angew. Chem., Int. Ed.*, 2005, **44**, 4345.
26 S. Vetrivel and A. Pandurangan, *J. Mol. Catal. A: Chem.*, 2004, **217**, 165.
27 J. Kim, S. Bhattacharjee, K. E. Jeong, S. Y. Jeong and W. S. Ahn, *Chem. Commun.*, 2009, 3904.

